Nuclear Import of Ho Endonuclease Utilizes Two Nuclear Localization Signals and Four Importins of the Ribosomal Import System*

Anya Bakhrat[‡1,2], **Keren Baranes**[‡1], **Oleg Krichevsky**[§3], **Inna Rom**[‡], **Gabriel Schlenstedt**[¶4], **Shmuel Pietrokovski**[∥5], **and Dina Raveh**[‡6]

From the Departments of ‡Life Sciences and §Physics, Ben Gurion University of the Negev, P. O. Box 653, 84105 Beersheba, Israel, the ¶Department of Medical Biochemistry and Molecular Biology, Saarlandes University, 66421 Homburg, Germany, and the ∥Department of Molecular Genetics, Weizmann Institute of Science, 76100 Rehovot, Israel

Activity of Ho, the yeast mating switch endonuclease, is restricted to a narrow time window of the cell cycle. Ho is unstable and despite being a nuclear protein is exported to the cytoplasm for proteasomal degradation. We report here the molecular basis for the highly efficient nuclear import of Ho and the relation between its short half-life and passage through the nucleus. The Ho nuclear import machinery is functionally redundant, being based on two bipartite nuclear localization signals, recognized by four importins of the ribosomal import system. Ho degradation is regulated by the DNA damage response and Ho retained in the cytoplasm is stabilized, implying that Ho acquires its crucial degradation signals in the nucleus. Ho arose by domestication of a fungal *VMA1* intein. A comparison of the primary sequences of Ho and fungal *VMA1* inteins shows that the Ho nuclear localization signals are highly conserved in all Ho proteins, but are absent from *VMA1* inteins. Thus adoption of a highly efficient import strategy occurred very early in the evolution of Ho. This may have been a crucial factor in establishment of homothallism in yeast, and a key event in the rise of the *Saccharomyces sensu stricto*.

Ho endonuclease initiates a mating type switch in *Saccharomyces cerevisiae* and related yeasts by making a site-specific double strand break in a 24-bp cognate site in the mating type gene, *MAT*. Repair of the double strand break is by gene conversion using one of the silent cassettes of mating type information (*HMLα* or *HMRa*) as a template. Repair occurs before replication of the *MAT* locus and each daughter cell has the new mating type with a regenerated Ho cognate site (1). Ho activity is tightly regulated: *HO* is transcribed briefly at the end of G$_1$, its transcription is restricted to haploid mother cells, *i.e.* cells that have divided at least once (2), and the protein is rapidly degraded by the ubiquitin-26 S proteasome system (3). Cells in which Ho is retained in

the nucleus beyond its normal time window of activity show perturbation of the cell cycle (4). Ho is marked for degradation by functions of the DNA damage response (DDR),[7] specifically the *MEC1*, *RAD9*, and *CHK1* pathway (5). Despite being a nuclear protein, Ho must exit the nucleus to be degraded in the proteasomes. The DDR functions are important for Ho phosphorylation: phosphorylation of threonine 225 is crucial for Ho nuclear export and additional phosphorylations are required for recruitment of Ho for ubiquitylation. Ho is ubiquitylated by the SCF (Skp1-Cdc53-F-box protein) E3 ubiquitin ligase complex, to which it is recruited by the F-box protein Ufo1 (6). In *mec1* mutants Ho is stabilized and accumulates in the nucleus; conversely trapping Ho in the nucleus by deletion of its nuclear exportin, Msn5, leads to stabilization of the protein (4). Ddi1 binds ubiquitylated Ho and is required for interaction of Ho with the proteasome; in its absence Ho is stabilized. The finding that Ho is not degraded within the nucleus, but in the cytoplasm, is further strengthened by the direct demonstration of accumulation of ubiquitylated Ho in the cytoplasm of Δ*ddi1* mutants (7).

Ho nuclear import is very rapid and efficient. Ectopic expression of *HO* leads to rapid cleavage of *MAT* (8), and to a mating type switch at any phase of the cell cycle in both mother and daughter cells. This indicates that there is no impediment to its nuclear import (9). Macromolecules are conveyed through nuclear pore complexes in the nuclear envelope by soluble karyopherins. Karyopherins comprise two structurally related families, α- and β-karyopherins. These recognize specific nuclear localization sequence (NLS) peptide motifs in the cargo molecule: NLSs may comprise a short stretch of basic residues (classical/cNLS), or two basic clusters 10–12 residues apart (bipartite NLS) (10). Cargoes may be recognized by an adaptor protein, α-karyopherin/Srp1, which mediates their binding to the transport receptor, β-karyopherin/Kap95 (11). Additionally, a family of about 14 β-karyopherins bind an array of cargoes directly and also makes contacts with the nucleoporin subunits of the nuclear pore complexes. Directionality of transport is determined by interaction with the GTPase Ran/yeast Gsp1. RanGTP is at a high concentration in the nucleus due to the asymmetric distribution of the Ran regulators. The nuclear guanine nucleotide exchange factor, RanGEF/yeast Prp20, converts RanGDP to RanGTP, whereas the GTPase activating protein, RanGAP/yeast Rna1, is localized in the cytoplasm and catalyzes the hydrolysis of RanGTP. Importin-cargo complexes assemble in the cytoplasm and after translocation into the nucleus they dissociate upon binding of RanGTP to the importin (12). To investigate how the efficient nuclear import that supports the unique biological function of Ho is achieved we located and analyzed its nuclear

import signals, and identified the nuclear importins that mediate its import.

Proteasomes and other components of the SCF are found throughout the cell and it is not clear why Ho cannot be degraded within the nucleus. One possibility is that it is not fully marked as a degradation substrate in the nucleus and needs to acquire additional phosphorylations by a cytoplasmic protein kinase. In this respect Ho may resemble the kinase inhibitor, Sic1, that requires multiple phosphorylations to reach a critical threshold for stable binding to its F-box receptor, Cdc4 (13). We therefore examined whether Ho acquires all the post-translational modifications that target it for degradation within the nucleus, or whether it can be marked as a proteasome substrate by a cytoplasmic protein kinase(s).

Homothallism in budding yeast arose by stepwise replications of the *MAT* locus leading to the establishment of three cassettes of mating type information. This was followed by acquisition of Ho by "domestication" of a fungal *VMA1* protein-splicing intein element (14–17). Intein protein domains are encoded by selfish genetic elements present within the protein coding regions of diverse genes. Inteins include a protein-splicing domain that catalyzes their extraction from the host polypeptide (18, 19). They typically also have an endonuclease domain that mediates copying of the intein gene into an orthologous unoccupied intein-integration point (20). Homology modeling of Ho based on the crystal structure of *S. cerevisiae* PI-SceI, a typical *VMA1* intein (21), indicates that Ho residues from the N-terminal domain (1–185) together with residues downstream of the endonuclease domain (428–465) form a protein splicing domain (with a small DNA recognition region between residues 93 and 157). The intervening region forms a LAGLIDADG-type homing endonuclease domain including all expected catalytic active site residues (16). In addition, Ho has a unique C-terminal 120-residue zinc finger domain (22) that is critical for mating type switching and may contribute to specificity of cognate site recognition (16, 23).

Despite their common ancestry Ho and PI-SceI have very different life strategies. PI-SceI is produced as part of the vacuolar ATPase protein precursor at all stages of the cell cycle, but is active only in meiotic cells (20). In contrast to Ho nuclear import that can occur in all cell types at all stages of the cell cycle (above), activity of the PI-SceI intein is regulated by its nuclear import. The spliced out intein is retained in the cytoplasm during vegetative growth and imported into the nucleus in premeiotic cells when the TOR (target of rapamycin) pathway is inactivated in response to nutrient depletion. Nuclear import of PI-SceI is mediated by the importin Srp1 (24). In diploids heterozygous for the intein, cleavage of the PI-SceI cognate site of the inteinless allele is followed by double strand break repair during which a copy of the endonuclease open reading frame is inserted at the cleaved site (homing). Homing disrupts the cognate site preventing further cleavage by the endonuclease (25). This is different from the repair of the *MAT* allele that regenerates the Ho cognate site during the mating type switch. To determine when the Ho nuclear import mechanism arose we therefore compared the protein sequences of Ho and PI-SceI from different Saccharomycete yeasts.

MATERIALS AND METHODS

Yeast Strains are described in Table 1.

Plasmid Construction

For two-hybrid clones, Gal4 activating domain fusions of Ho and subclones were constructed by R. Buchnik using restriction fragments (56). The PseI-DNA binding domain fusion in pOBD was obtained from Peter Uetz (26). Construction of pYES2-*HO* and *HO* and *HO C508A*,*C511A* in pHY315-GFP are described in Ref. 16. GFP-NLS1 was made by amplifying a fragment centered around the NLS1 of *HO* with primers NLS1Not1F (GAGAAAATGCGGCCGC-CTGGGGTCTCTACCTTACG) and NLS1Sac1R (CGAACTTCTAT-GAGCTCGCCGTACATAAATTCAGGG). The PCR product was digested with NotI and SacI and introduced in-frame to GFP in pHY315-GFP. *HO* NLS2 was amplified using primers NLS2F (GCT-TCACTAGTGATTTCCAGGGTGAGAG) and HoSac1R (CAGAT-GAGCTCACCTGCGTTGTTACCACAAC). The PCR product was digested with SpeI and SacI and cloned into pHY315-GFP. HOΔNLS1 was constructed by overlap primer extension using primer pairs: HoSpe1F and ΔNLSClaR (CGTAAGATCGATACCCCAGATTTTTC GC), and HoSac1R and ΔNLSClaF (GCAAATCGATGAATTTATG-TACGGCGAG). Deletion of NLS2 employed primer pair ΔNLS2F (GAACAGGATTGGAGTGGTAAAAATCG) and ΔNLS2R (CCA-ATCCTGTTCTCCCACACAGCAGC); mutation of NLS2 residues, HoR491A,K492A employed primer pair NLS2 RKF (CCCGCGGCCG-GAATCAAGTATTTTTATAAAGATTGG) and NLS2 RKR(TCCG-GCCGCGGGACAAGCAACACAGTGTTTTAGATTC). The final PCR products were cloned as above. The *KAP123-GFP* strain was constructed by integration of a GFP PCR fragment before the stop codon of the gene by homologous recombination (27). Mating conditions and tester strains are as described in Ref. 16.

For microscopy, GFP fusion proteins were produced by overnight growth in SD medium with 2% galactose and observed using a Nikon TE300 fluorescence microscope fitted with a GFP-specific filter set: dichroic 505 nm, excitation 450–490 nm, emission (low pass) 515 nm (Nikon). Images were captured with a Micromax 512 BFT digital camera (Roper Scientific) using WinView32 imaging software and analyzed with image processing routines in the MatLab environment. To determine the subcellular localization of Ho, NLS1, and NLS2 in wild type and each karyopherin mutant we analyzed cells according to the following procedure: three regions of interest corresponding to nucleus, cytoplasm, and adjacent cell background were chosen and the pixel value for each region (N, nucleus; C, cytoplasm; B, background) was used to determine the nuclear/cytoplasmic ratio for each cell. A ratio for each cell sampled was calculated using (N-B)/(C-B). Based on this we calculated the median ratio for each cell population. Table 2 shows the median values of the nuclear/cytoplasmic ratio for Ho, NLS1, and NLS2 in wild type and mutant cells. For temperature-shift experiments, cultures after overnight induction were shifted to 37 °C with continuous induction for a further 2 h.

Co-immunoprecipitation-Immunoblotting

Yeast cells were grown overnight to late logarithmic phase (A_{600} = 0.8) in 50 ml of the appropriate inductive synthetic minimal medium with 2% galactose for expression of *GAL-HO*. The cells were harvested by centrifugation, washed in 50 ml of TE, and resuspended in 400 μl of co-IP buffer (0.1% Nonidet P-40, 250 mM NaCl, 5 mM EDTA, 50 mM Tris-Cl, pH 7.5, 1:25 of Boehringer Protease Inhibitor mixture). 0.5–0.6-g Glass beads were added and cells were broken with a glass beater (Biospec Products) using five 1-min cycles at 4 °C. The lysate was clarified by centrifugation at 13,000 × *g* for 15 min at 4 °C and protein concentration was measured with the Bio-Rad protein reagent. 5–15 mg of protein lysate were used for IP with the appropriate antibodies in co-IP buffer at 4 °C for 1–2 h with mild shaking. 30 μl of 50% Protein A-Sepharose (Amersham Biosciences) were added to each sample and incubation was continued under the same conditions for 0.5–1 h. The samples were washed 6 times with co-IP buffer with 1% Triton. The pellet was resuspended in 30 μl of 2× Laemmli sample buffer, boiled for

TABLE 1

Yeast strains with karyopherin mutations

PSY strains were obtained from J. Hood (55), others were purchased from Euroscarf. Mating tester strains were DC14 (*MAT***a**, *his1*) and DC17 (*MAT*α, *his1*) (8).

PSY688	*srp1-31, ura3, leu2, trp1, his3, ade2*	α
PSY713	*prp20-1, ura3-52, leu2Δ1, trp1 Δ63*	α
PSY714	*rna1-1, ura3-52, leu2Δ1, trp1*	**a**
PSY716	*yrbl::HIS3, ura3, trp1, pCEN LEU yrb1-1*	**a**
PSY967	*kap123::HIS3, ura3-52, leu2Δ1, his3 Δ200*	**a**
PSY1040	*cse1, ura3-52, ade2-101, his3-11, 15 trp1Δ901*	α
PSY1102	*rsl1-3, ura3-52, leu2Δ1, trp1 Δ63*	**a**
PSY1105	*xpo1::LEU2, ade2-1, ura3-1, trp1-1, can1-1, + pKW457 (pCEN xpo1-1 HIS3)*	α
PSY1136	*msn5::HIS3, leu2Δ1, ura3-52, his3 Δ200*	α
PSY1199	*nmd5::HIS3 ura3, leu2, trp1, his3*	α
PSY1200	*sxml1::HIS3, leu2Δ1, his3Δ200, trp1 Δ63, ura3-52*	**a**
PSY1201	*pse1-1, ura3-52, leu2 Δ1, trp1 Δ63*	*a*
BY4741	*his3Δ1, leu2 Δ0, met15Δ0, ura3Δ0*	
B0062A	YBR017c/*kap104::URA3 CEN, PK; ura3-52, his3Δ1, leu2, 3-11, 2, trpI-289*	
Y04608	YGL241w/*kap114::kanMX4, his3Δ1 leu2Δ0, met15Δ0 ura3Δ0*	a
Y02127	YPL125w/*kap120::kanMX4, his3Δ1, leu2Δ0, met15Δ0, ura3Δ0*	a
Y04384	YGL016w/*kap122::kanMX4, his3Δ1, leu2Δ0, met15Δ0, ura3Δ0*	a
Y00000-*BY4714*	*his3Δ1, leu2Δ0, met15Δ0, ura3Δ0*	a

10 min, and electrophoresed on a 10% polyacrylamide SDS gel (PAGE) with protein size standards. The gel was transferred to nitrocellulose membrane (Protran BA 85, Schleicher & Schuell) and Western blotting was performed with the appropriate antisera. 1 mg of crude protein was used to determine input by IP-Western blot and 30 μg was taken for direct Western blotting.

For determination of Ho half-life cells were induced as above. For promoter shutoff 3% glucose was added at the zero time point, together with cycloheximide to a final concentration of 10 mM to inhibit translation. Aliquots were collected at the times indicated for anti-GFP immunoprecipitation and Western blotting as described above.

For Pulldown Experiments—GST fusion proteins were produced in logarithmic bacterial cultures by overnight incubation with 0.1 mM isopropyl 1-thio-β-D-galactopyranoside at 20 °C. The cells were pelleted by centrifugation at $3,500 \times g$ in a Sorvall centrifuge, resuspended in 10% phosphate-buffered saline with 0.5% Nonidet P-40 and 1:25 of Boehringer Protease Inhibitor mixture, and sonicated. The lysate was clarified by centrifugation at $12,000 \times g$ for 10 min. Lysates from 1-liter cultures were incubated with 150 μl of GSH beads for 60 min at 4 °C. The beads were washed three times in lysis buffer. Yeast lysates were prepared as above, 10 μl of conjugated GSH beads were incubated with 300 μl of yeast lysate in a pulldown experiment for 90 min at 4 °C. The bead pellet was washed three times with yeast co-IP buffer and then separated by SDS-PAGE for immunoblotting as above.

6His-Pse1p and 6His-Gsp1p—6His-Pse1p and 6His-Gsp1p were purified with nickel-nitrilotriacetic-agarose (Qiagen). Pse1p was further purified by Mono Q (Amersham Biosciences) chromatography. The GTP-bound form of 6His-Gsp1p was separated on a Mono S column (Amersham Biosciences) and the GTP/GDP contents were determined by high pressure liquid chromatography analysis. The Gsp1p-GTP preparation contained 50% GTP-bound protein.

Antibodies were purchased from Santa Cruz Biotechnology and used at the following dilutions: anti-GFP, 1:200 for immunoprecipitation and 1:1000 for Western blotting; anti-LacZ and anti-His, 1:600 for immunoprecipitation and 1:1000 for Western blotting; anti-GST, 1:5000 for Western blotting; goat anti-rabbit and goat anti-mouse at 1:1000 for Western blotting. Detection was by ECL using an Amersham Biosciences ECL Western blotting kit.

Phylogenetic Analysis and Sequence Data

Multiple sequence alignments were calculated by the BlockMaker (28) and dialign2 (29) programs. Sequence logos, showing the multiple alignment conservation, were calculated according to Ref. 28. Phyloge-
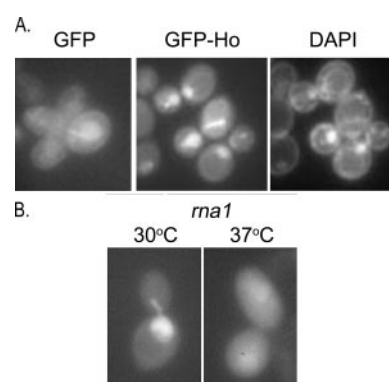

FIGURE 1. *A*, fusion of Ho to GFP leads to nuclear accumulation of GFP that by itself gives a diffuse cytoplasmic signal. 4′,6-Diamidino-2-phenylindole (*DAPI*) stain showing nuclei that coincide with the GFP-Ho signal. *B*, GFP-Ho nuclear import is impaired in the *rna1* (RanGAP) mutant at the restrictive temperature.

netic trees were calculated with the PHYLIP program (30). A consensus tree was made from neighbor joining trees calculated from protein distance matrices of 1000 bootstrapped sequence versions, using default program parameters. NCBI data base accessions of the Ho sequences analyzed are *Saccharomyces cerevisiae* 1431383, *Saccharomyces pastorianus* HO-Sc 7576368, *S. pastorianus* HO-Lg7576436, *Saccharomyces bayanus HO*-1 7576438, *S. bayanus HO*-2 29365020, *Saccharomyces mikatae* 9364028, *Saccharomyces paradoxus* 22830763, *Saccharomyces castellii* 30988068, *Saccharomyces kudriavzevii* 30995262, *Kluyveromyces delphensis* 42557539, *Candida glabrata* 42557533, and *S. castellii* Ho-like 30988030. The full sequence of *Zygosaccharomyces rouxii* Ho was kindly provided by Ken Wolfe, University of Dublin. Sequences of the fungal *VMA1* inteins are available on the NEB intein data base (31) including those we identified and deposited there.

RESULTS

Identification of Karyopherins and NLSs Involved in Nuclear Import of Ho—The subcellular location of Ho was directly visualized by fusing it to GFP. We screened mutants in the karyopherins Srp1, Rsl1/Kap95, Kap104, Kap114, Kap120, Pse1/Kap121, Pdr6/Kap122, Yrb4/Kap123, Nmd5, Sxm1, Cse1, Xpo1, and Msn5; in Prp20 (RanGEF) and Rna1 (RanGAP), and in a mutant of the Ran-binding protein Yrb1 (Table 1). Conditional mutants were used to test essential genes. We found Ho in the nucleus of wild type cells (Fig. 1*A*) and in all the karyopherin mutants screened above. In *rna1* mutants nuclear import of GFP-Ho was severely impaired at the restrictive temperature indicating that Ho
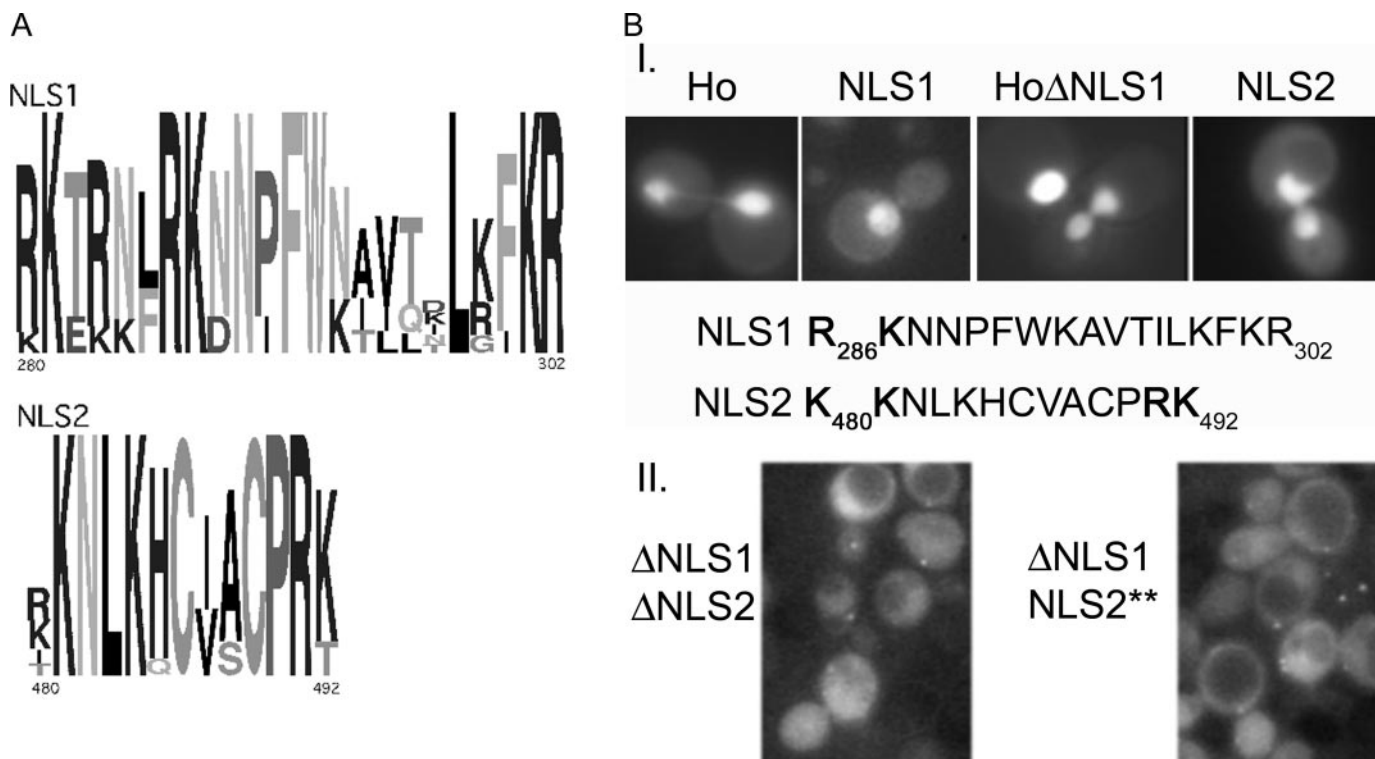
A

NLS1

NLS2

B

I.

NLS1 R$_{286}$KNNPFWKAVTILKFKR$_{302}$

NLS2 K$_{480}$KNLKHCVACPRK$_{492}$

II.

ΔNLS1
ΔNLS2

ΔNLS1
NLS2**

FIGURE 2. *A*, sequence logos of *Saccharomyces* Ho NLS1 and NLS2 regions. The conservation of residues at each position is indicated by the *height of the letter* designating that residue. The start and end positions of each NLS in *S. cerevisiae* are indicated; residues from Arg-280 to Lys-302 are included in this analysis, the actual NLS1 may start at Arg-286. *B: I*, GFP-Ho is nuclear (*Ho*); HoNLS1 imports GFP into the nucleus (*NLS1*). Deletion of NLS1 does not affect nuclear import of GFP-Ho (*HoΔNLS1*) and this version of Ho gives a strong nuclear signal. HoNLS2 imports GFP into the nucleus (*NLS2*). The amino acid sequences of the two bipartite Ho NLS1 and NLS2 sequences of *S. cerevisiae* are shown with the basic residues emphasized. *II*, deletion of both NLS1 and NLS2 prevents nuclear import of Ho indicating that *in vivo* these two NLSs mediate Ho nuclear import. The same result is obtained by deletion of NLS1 combined with mutation of 2 basic residues of the bipartite NLS2, R491A,K492A (*NLS2***).

import depends on Ran (Fig. 1*B*). In parallel we assayed a series of isogenic wild type and yeast mutants for their ability to support a mating type switch. *HO* was induced from the *GAL* promoter in p*YES2-HO* and the cells were mated with a tester of the opposite mating type to test for their mating efficiency, and with a tester of their original mating type to test for a mating type switch. *rna1* mutants did not switch, however, all the karyopherin mutants switched mating type, indicating that nuclear import of Ho was not abrogated by deletion of any single karyopherin. These results imply functional redundancy between the karyopherins that mediate Ho nuclear import and/or the existence of more than one NLS on Ho imported by different karyopherins.

The Ho sequence shows a putative bipartite NLS between residues 280 and 302. This region is highly conserved in Ho from different species, in particular the crucial basic residues (Fig. 2*A*). In the past we reported that mutation of Arg-286 abrogates mating type switching in yeast (16). Arg-286 aligns with PI-SceI Asn-281, a residue that contacts the DNA in the cocrystal (32). We fused Ho residues 248–311, centered around this putative NLS (NLS1), to GFP and found that this Ho fragment led to nuclear accumulation of GFP. However, when we deleted NLS1 from Ho this did not affect Ho nuclear import. Further inspection of the primary sequence indicated another very well conserved putative bipartite NLS in the zinc finger domain between residues 480 and 492 (Fig. 2). Indeed fusion of residues 441–596 (NLS2) to GFP led to accumulation of GFP in the nucleus (Fig. 2*B*). This supports an earlier observation that mutation of cysteine residues in the zinc finger domain of Ho besides leading to loss of Ho activity greatly reduces nuclear accumulation of GFP-Ho (16). We deleted both NLS1 and NLS2 regions (residues 286–302 and 480–496) and found that the resulting Ho protein was not imported at all into the nucleus in wild type cells. Similarly the above

NLS1 deletion combined with NLS2 point mutations of R491A,K492A also abrogated nuclear import, indicating that it is the basic residues of the NLS that are important for binding the karyopherin (Fig. 2*B*). These experiments indicate that we have correctly delineated the functional NLSs of Ho.

Having identified two NLSs in Ho we rescreened the karyopherin mutants for their ability to import GFP-Ho, and each GFP-NLS1 and GFP-NLS2, separately. GFP-NLS1 nuclear import was reduced in *pse1* mutants at the restrictive temperature as evidenced by the ratio of nuclear to cytoplasmic GFP signal; GFP-NLS1 was also predominantly cytoplasmic in *kap123* mutants. In addition in *sxm1* mutants GFP-NLS1 showed a relatively high cytoplasmic signal compared with GFP-NLS2. Nuclear import of GFP-Ho and GFP-NLS2 was not affected in *pse1*, *kap123*, or *sxm1* mutants; the only mutant in which GFP-NLS2 was predominantly cytoplasmic was *kap120* (Fig. 3 and Table 2). Although they could support a mating type switch, microscopic observation of *nmd5* mutants revealed a general import defect that severely reduced nuclear import of GFP-Ho, GFP-NLS1, and GFP-NLS2 (not shown) and were not analyzed further.

Interaction of Karyopherins with Ho—To further support the GFP-Ho nuclear import data we tested for an interaction between Ho and PseI in the two-hybrid protein interaction trap. Full-length Ho, and a number of subclones (Fig. 4*A*) were fused to the Gal4 activation domain in plasmid pGAD424 (Clontech) and co-transformed into reporter strains (33) together with plasmids expressing *PSE1* fused to the Gal4 DNA binding domain (pOBD) (26). Transformants in which Ho interacted with PseI activated the *GAL1-HIS3* and *GAL2-ADE2* reporter genes and grew on the selective plates. Ho, residues 1–566, and Ho subclone 186–441 interacted with PseI. However, subclones encompassing residues 1–297, 299–565, and 441–566 did not interact. This analysis confirmed
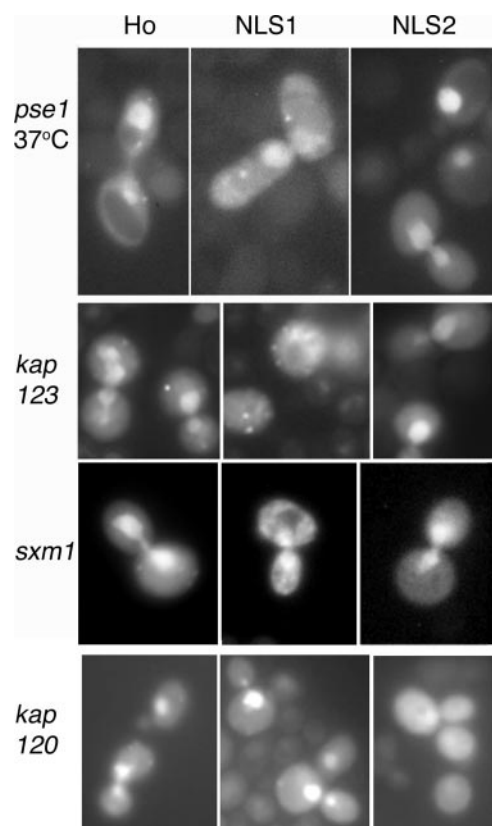
FIGURE 3. **Import of GFP-Ho, GFP-NLS1, and GFP-NLS2 into the nucleus in *pse1*, *kap123*, *sxm1*, and *kap120* mutants.** The strongest effect on nuclear import of GFP-NLS1 is observed in *kap123* mutants where the nuclear accumulation observed in cells expressing GFP-Ho and GFP-NLS2 is not observed for GFP-NLS1. *pse1* and *sxm1* mutants show a higher cytoplasmic signal for NLS1 than for either Ho or NLS2. In *kap120* mutants GFP-Ho and GFP-NLS1 show a strong nuclear signal but there is no nuclear accumulation of GFP-NLS2. Ratios of nuclear/cytoplasmic signals for these three GFP fusion proteins in the four karyopherin mutants are summarized in Table 2.

TABLE 2

Nuclear/cytoplasmic ratio ($R \pm E$) for Ho, NLS1, and NLS2 in wild type and karyopherin mutant cells

R is the median of multiple measurements $\{R_i\}$ on the same type of cells: $R = median$ $\{R_i\}$. Errors (E) are estimated by median square deviation of the data from the median, $E = \sqrt{median\{(R_i - R)^2\}}$. The number of cells analyzed appears in parentheses.

Strain	Ho	NLS1	NLS2
WT	2.9 ± 0.7 (23)	2.2 ± 0.4 (36)	2.4 ± 0.6 (18)
pse1 37 °C	2.4 ± 0.5 (38)	1.8 ± 0.3 (21)	2.6 ± 0.6 (39)
kap123	2.0 ± 0.4 (38)	1.0 ± 0.1 (20)	1.9 ± 0.2 (14)
sxm1	1.9 ± 0.3 (24)	1.4 ± 0.2 (15)	1.8 ± 0.2 (24)
kap120	1.6 ± 0.1 (20)	1.8 ± 0.3 (18)	1.2 ± 0.2 (13)

the bipartite NLS1 sequence we identified between residues 280 and 302. This NLS would be intact in the interacting subclones, but split in clones 1–297 and 299–565. NLS2 is between residues 480 and 496 and our observations on nuclear import of GFP-NLS2 indicated that its import is indeed not affected in *pse1* mutants (Fig. 3).

In contrast to α-karyopherins that form a heterodimer with a nucleoporin-binding β-karyopherin, Kap95, subunit, most β-karyopherins bind both their cargo and the nucleoporin subunits. However, it was recently reported that the nucleolar protein Sof1, a cargo of PseI, does not bind PseI directly. Instead Sof1 employs a NopI bridge that mediates its nuclear import via PseI by a "piggyback" mechanism (34). We therefore tested whether Ho interacts directly with PseI using recombinant proteins expressed in *Escherichia coli*. Full-length Ho (residues 1–586) and a C-terminal truncation of Ho that extends from residues 1 to 451 were fused to GST and isolated on glutathione-Sepha-
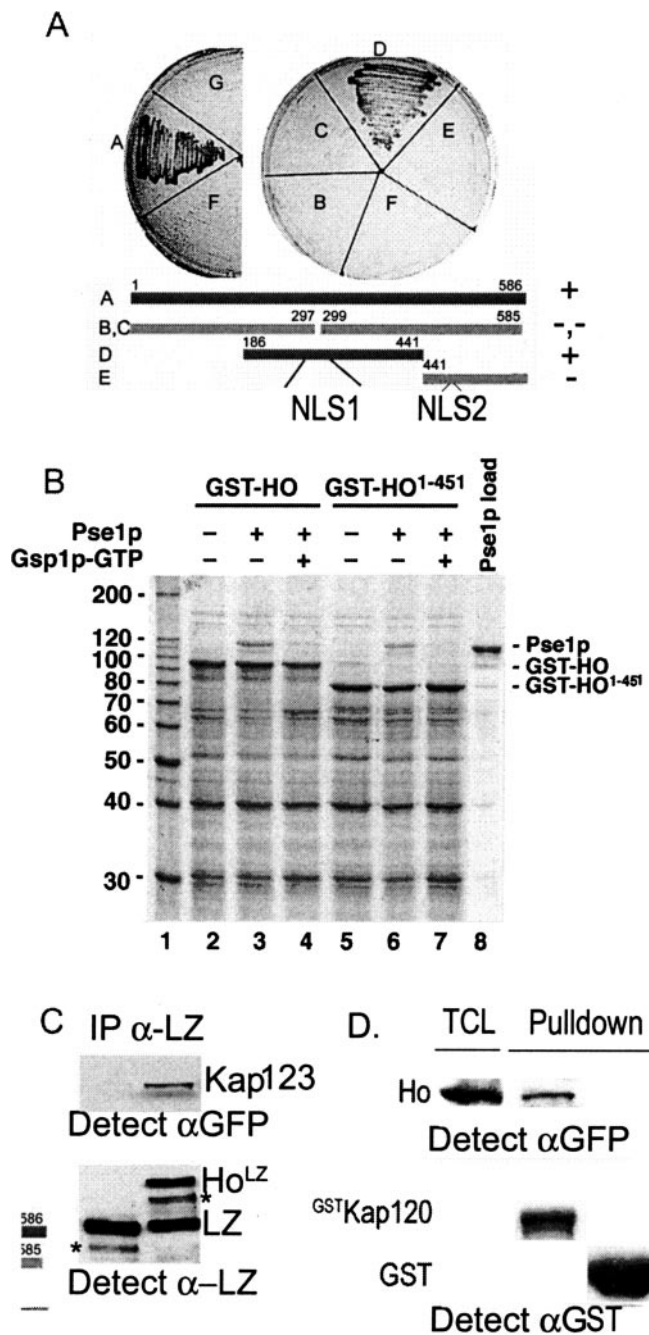
FIGURE 4. *A*, delineation of Ho NLS1 by two-hybrid experiments between subclones of Ho fused to the Gal4 DNA binding domain (*BD*) and PseI to the activating domain (*AD*). Full-length Ho (*A*) and fragment D interact with PseI. F, Ho/BD vector, and G, Pse1/AD vector controls. Fragments B and C do not include an intact NLS1 and do not bind PseI. Fragment D has a complete NLS1 and binds PseI. Fragment E does not encompass NLS1 and does not bind PseI. We subsequently mapped NLS2 to this fragment. *B*, recombinant PseI interacts directly with full-length recombinant Ho and with Ho truncated after residue 451. *Lane 1*, marker; *lane 2*, GST-Ho; *lane 3*, GST-Ho-PseI interaction; *lane 4*, the GST-Ho-PseI reaction is abrogated in the presence of Gsp1GTP; *lane 5*, GST-Ho$^{1-451}$; *lane 6*, GST-Ho$^{1-451}$-PseI interaction; *lane 7*, GST-Ho$^{1-451}$-PseI interaction is abrogated by addition of Gsp1GTP; *lane 8*, PseI. *C*, Ho interacts with Kap123 by co-immunoprecipitation. Cotransformants expressing *KAP123-GFP* and *HO-LACZ* (molecular mass 180 kDa) or *LACZ* (molecular mass 130 kDa) alone were immunoprecipitated with anti-LacZ. Kap123-GFP (molecular mass 149 kDa) was detected by Western blotting with anti-GFP (*top*) and inputs are shown with anti-LacZ. *Asterisk* marks LacZ degradation product. *D*, Ho interacts with Kap120 in a pulldown experiment. Yeast lysates from cells that produced GFP-Ho were incubated with GSH beads to which GST-Kap120 (molecular mass 159 kDa) or GST were conjugated. After washing the bead fractions were analyzed by SDS-PAGE and Western blotting with anti-GFP serum to detect Ho, and with anti-GST serum to detect the conjugated proteins on the beads. *TCL* is total cell lysate.
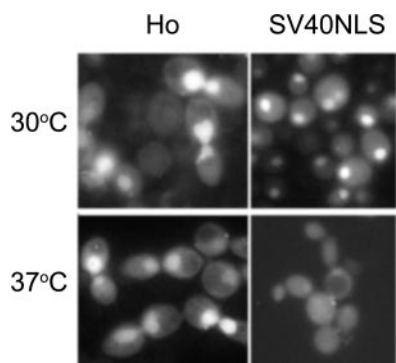
FIGURE 5. **Ho is nuclear in *srp1* mutants at both the permissive (30 °C) and the restrictive (37 °C) temperatures.** Nuclear import of a control Srpl binding NLS derived from SV40 is abrogated at 37 °C indicating that the SrpI function is indeed lost in the mutant at this temperature.

FIGURE 6. **Phylogenetic tree of Ho and fungal *VMA1* inteins.** A multiple alignment of 145 ungapped certainly aligned positions of Ho and *VMA1* fungal inteins was used to construct the tree. The tree was rooted by including the *Debaryomyces hansenii* GLT1 intein as an out group. Percent bootstrap values are shown for selected nodes. Sequences are named HO, HO-like, or PI (inteins, for protein introns) and the species designations are: *Cgl, C. glabrata; Ctr, C. tropicalis; Dha, D. hansenii; Kde, K. delphensis; Kla, K. lactis; Kpo, Kluyveromyces polysporus; Lel, Lodderomyces elongisporus; Pst, Pichia stipitis; Sce, S. cerevisiae; SceDH1, Saccharomyces species; DH1–1A, Sba, S. bayanus; Scar, Saccharomyces cariocanus; Sca, S. castellii, Sda, Saccharomyces dairenensis; Sex, Saccharomyces exiguous; Sku, S. kudriavzevii; Smi, S. mikatae; Spar, S. paradoxus; Spa, S. pastorianus; Sun, Saccharomyces unisporous; Tgl, Torulaspora globosa, Tpr, Torulaspora pretoriensis; Zba, Zygosaccharomyces bailii; Zbi, Zygosaccharomyces bisporus; Zro, Z. rouxii.*

rose beads. PseI fused to a His$_6$ tag was purified from a bacterial lysate and incubated with the column material. PseI was retained in the presence of Ho, but not by the beads control. It was released from the column by Gsp1GTP (RanGTP). This result indicates that PseI interacts directly with Ho. In our two-hybrid experiments PseI did not interact with clones of Ho derived from the C-terminal part of the protein, residues 441–565. Likewise in the *in vitro* experiments PseI interacted with the full-length Ho protein and with a protein truncated at residue 441 (Fig. 4*B*). To test the interaction between Ho and Kap123 we transformed *pTET-HO-LACZ* and *pTET-LACZ* (3) into cells that express *KAP123-GFP* from the *KAP123* promoter and immunoprecipitated Ho-LacZ and control LacZ with anti-LacZ antiserum. Western blotting with anti-GFP showed that Ho-LacZ binds Kap123; binding is via the Ho moiety as the LacZ control did not bind Kap123 (Fig. 4*C*). In a pulldown experiment in which yeast lysate from cells producing GFP-Ho was incubated with GST-Kap120 and GST controls on GSH beads we found that Kap120 binds Ho, whereas the GST control beads do not (Fig. 4*D*). These protein-protein interaction assays show a correlation with the data obtained by direct visualization of the GFP fusion proteins.

The Ho NLSs Arose Early in Its Domestication—Ho arose by domestication of a fungal *VMA1*-type intein, exemplified by the well studied PI-SceI (14–17). The Ho protein in all species of *Saccharomyces* is extremely highly conserved. This Ho protein has retained the intein protein splicing, homing endonuclease, and DNA binding domains, and acquired a unique zinc finger region. NLS1 is in the endonuclease domain, whereas NLS2 is in the zinc finger domain. PI-SceI is imported into the nucleus by the α-importin, SrpI (24). Here we found that at the restrictive temperature for *srp1–31*, Ho is nuclear, indicating that SrpI is not required for nuclear import of Ho. A control bipartite NLS derived from the cNLS of SV40 (35) remains in the cytoplasm indicating that SrpI activity is indeed lost in the mutant (Fig. 5). We compared the Ho and VMA1-type inteins to examine the origin of the two Ho NLSs. The region corresponding to Ho NLS1 (PI-SceI-(275–297)) does not have any NLS features and is not conserved in different yeast *VMA1* inteins (results not shown). In structures of PI-SceI this region forms a surface patch and its N-terminal half becomes ordered upon co-crystallization with the endonuclease DNA target (32). Inspection of other fungal inteins (such as those of the PRP8 proteins (36)) did not identify any conserved NLS-like regions in their endonuclease domains. The additional NLS of Ho, NLS2, is in the zinc finger domain of Ho, the domain unique to Ho and not present in inteins. We compared the common sequence regions of Ho and the VMA1-type inteins (all domains apart from the zinc fingers) and found that the Ho proteins and fungal
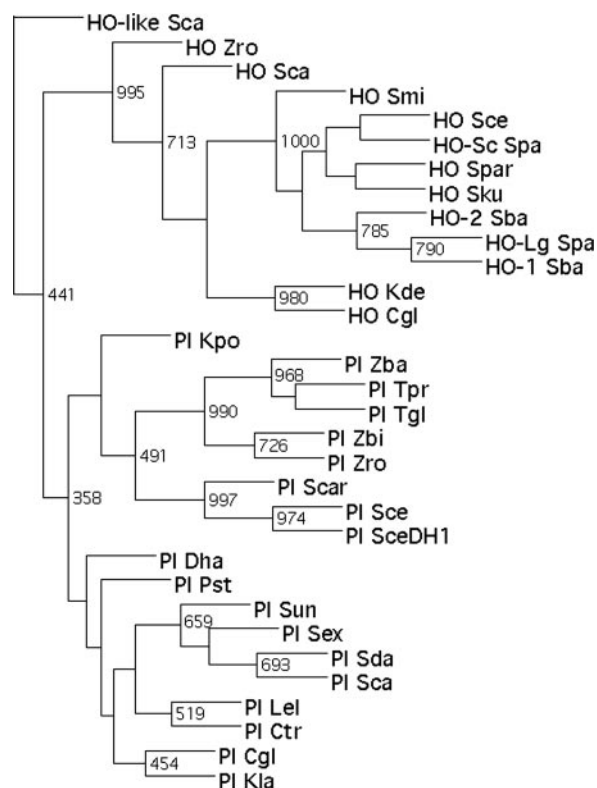
VMA1-type inteins form two separate groups (Fig. 6). The Ho protein closest to the divergence point is that of *Z. rouxii*, a species that did not undergo genome duplication but is closer to species that have acquired Ho than to those that have not (37). This phylogenetic analysis shows that the efficient nuclear import of Ho is based on two NLSs acquired after divergence from its intein ancestor.

Disruption of Ho Nuclear Import Stabilizes the Protein—The sensitivity of Ho activity to mutation in the regions of NLS1 and NLS2 (16) precluded the use of mating type switching as a functional bioassay for mutational analysis of the putative NLSs. We therefore devised an alternative functional assay based on our findings that Ho is marked as a proteasome substrate within the nucleus by functions of the DDR and is then exported to the cytoplasm to be degraded (3, 4, 7). These experiments while showing that Ho nuclear export is essential for its degradation, did not address the question of whether Ho acquires additional phosphorylations in the cytoplasm. Lack of nuclear import of Ho could perhaps direct it for rapid degradation due to its mislocalization, or alternatively if the crucial modifications that mark Ho as a proteasome substrate occur exclusively within the nucleus this could extend its half-life. Here delineation of the Ho NLSs and the karyopherins that mediate its nuclear import allow us to address this question. We previously reported that mutation of two upstream cysteine residues of each of the putative zinc fingers of Ho abolished mating type switching. These Ho mutants showed reduced nuclear import, although in Δ*msn5* mutants it
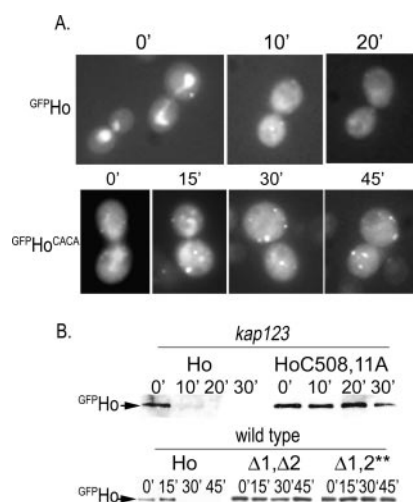
FIGURE 7. *A*, half-life of Ho (GFPHo) and Ho(C508A,C511A). GFPHoCACA, in a *kap123* mutant determined by microscopy after translation shutoff at the zero time point. The GFP-Ho signal is nuclear at the zero time point, but 10 min after addition of cycloheximide there is no longer a nuclear GFP-Ho signal and by 20 min there is no GFP signal in these cells. Cells expressing Ho(C508A,C511A) have a strong GFP cytoplasmic signal and during the course of the experiment, a large part of the cytoplasmic signal accumulates in discrete spots, probably aggresomes. *B*, *top panel*: half-life of Ho and Ho(C508A,C511A) in a *kap123* mutant determined by translation shutoff and immunoprecipitation of aliquots at the designated time points followed by Western blotting with anti-GFP antiserum. *Lower panel*: half-life of GFP-Ho (*Ho*), GFP-HoΔNLS1,ΔNLS2 (*Δ1,Δ2*), and GFP-HoΔNLS1,NLS2(R491A,K492A) (*Δ1,2***) in wild type cells determined as described above.

was possible to accumulate some GFP-Ho within the nucleus (16). Based on our results above this nuclear import can now be attributed to the activity of NLS1 as the zinc finger mutations probably affect NLS2 (residues 480–492)-mediated nuclear import. We therefore expressed the zinc finger mutant, Ho (C508A,C511A), in a Δ*kap123* mutant that recognizes NLS1, to investigate the half-life of Ho misdirected to the cytoplasm. We produced GFP-Ho and GFP-Ho(C508A,C511A) by growing the cells in galactose for 18 h and added 10 mM cycloheximide at the zero time point to inhibit further translation of *HO* mRNA. We found that in *kap123* mutants native Ho whose nuclear import is supported by NLS2, is degraded normally: by 10 min the GFP-Ho signal is no longer nuclear, it is very weak and after 20 min the GFP-Ho signal disappears totally. In contrast in the *kap123* mutants in which GFP-Ho(C508A,C511A) is cytoplasmic the protein is stabilized. From the zero time point onwards we observed a diffuse GFP-Ho signal throughout the cytoplasm together with high level GFP fluorescence in peripheral spots that probably correspond to aggresomes. The GFP-Ho(C508A,C511A) signal remained bright indicating that Ho was not degraded throughout the hour of the experiment. At no time was there any evidence of vacuolar accumulation of Ho (Fig. 7*A*). Direct determination of the half-life of GFP-Ho and GFP-Ho(C508A,C511A) remaining at different times after addition of cycloheximide to the growth medium, by immunoprecipitation and Western blot analysis, confirmed that the mutant protein that did not enter the nucleus was stabilized. Ho was rapidly degraded in *kap123* mutants, whereas Ho(C508A,C511A) did not undergo any degradation during the 40 min of the experiment (Fig. 7*B*). Further experiments employing wild type cells showed similar stabilization of Ho deleted for both NLS1(Δ286–302) and NLS2(Δ480–496); and for Ho deleted for NLS1 and mutated in the basic residues of NLS2 (R491A,K492A), neither of which are imported into the nucleus (Fig. 7*B*). (Deletion of NLS1 does not include the PEST degron that determines the half-life of Ho, situated between residues 216 and 236 (3)). These results indicate that when Ho does not follow its regular pathway of nuclear import and accumulates in the cytoplasm it is protected from the ubiquitylation machinery that mediates its rapid degradation.

DISCUSSION

Our experiments demonstrate that efficient nuclear import of Ho is achieved through two separate bipartite NLSs and involves at least four different importins. Functional redundancy is a hallmark of yeast karyopherins as only four β-karyopherins are encoded by essential genes (11). The nuclear import observations of GFP fusion proteins suggest that NLS1 in the endonuclease domain of Ho is recognized chiefly by Kap123. However, the two-hybrid and *in vitro* binding experiments show a strong interaction with PseI too. In fact the two-hybrid Ho subclones that interacted with PseI enabled precise delineation of NLS1. Kap123 and PseI are the major importins of ribosomal proteins (38, 39). Kap123 is not essential for growth due to its functional redundancy with PseI and SxmI, each of which complements growth of *kap123* mutants (38–40). Kap123 and PseI are also crucial for export of mRNA; here too the synthetic lethality of *kap123*, *pse1* mutants can be suppressed by overexpression of *SXM1* (41). We find the same functional redundancy between Kap123, PseI, and SxmI in Ho import via NLS1. Ribosomal biosynthesis imposes a considerable metabolic burden on actively growing yeast cells (42) and use of the functionally redundant highly abundant ribosomal importins by Ho has doubtless contributed to the evolution of Ho activity in yeast. Proteins that function in the same pathway are often imported by the same karyopherin whose abundance may fluctuate during the cell cycle. In this context it is interesting to find that a major importin of Ho, PseI, also mediates import of Ste12 required for yeast mating (43). Identification of the Ho bipartite NLS1 as the signal recognized by PseI is the first characterization of a NLS recognized by this karyopherin. In a previous report (16) we showed that mutation of Arg-286 to alanine abrogates a mating type switch. This residue was chosen for mutagenesis as our structural model of Ho indicated that the parallel residue, Asn-281, is essential for PI-SceI activity and indeed contacts the DNA. Arg-286 is part of NLS1 of Ho and our present analysis in which we show that in the absence of NLS1, Ho nuclear import is supported by NLS2, confirms that it is the effect of the point mutation R286A on Ho activity and not on its nuclear import that leads to abrogation of mating type switching. Given the sensitivity of Ho activity to mutation we used native Ho in all our mating type tests of karyopherin mutants. PseI and Kap123 also import the histone acetyltransferase complex, SAS-1, however, the consensus NLS signal derived from these experiments and a bioinformatics analysis of other putative cargoes of this importin (44) does not resemble NLS1 of Ho.

The zinc finger region of Ho, unique among LAGLIDADG endonucleases, provides a second bipartite NLS recognized by Kap120. Interestingly Kap120 too has been identified as a karyopherin of ribosomal proteins (45). Here our mutational analysis shows that Kap120 binds a bipartite NLS. We previously showed that mutations in the zinc finger domain of Ho lead to loss of mating type switching. This is due to the effect of the mutations on Ho structure as using a Δ*msn5* mutant in which Ho nuclear export is inhibited, we showed that Ho with mutations in this region of the protein does enter the nucleus (16). Based on the results presented here we conclude that this nuclear import is mediated by NLS1, as in *kap120* mutants it is only nuclear import of GFP-NLS2 that is affected, both GFP-Ho and GFP-NLS1 are imported into the nucleus. Therefore acquisition of a unique zinc finger domain with NLS2 further increased the efficiency of Ho import. Use of multiple importins each present in copious amounts (46) can explain the high efficiency of Ho import.

The identification of the Ho nuclear import machinery enabled us to

revisit the role of the DDR phosphorylations in targeting Ho for degradation in the proteasome. We find that when its nuclear import is abrogated Ho is stabilized. We hypothesize that in the cytoplasm Ho is not recognized and marked as a degradation substrate. In this respect Ho turnover may resemble the G_0-G_1-specific degradation of the cyclin-dependent kinase inhibitor, $p27^{KIP}$, which occurs in the cytoplasm. At this stage of the cell cycle $p27^{KIP}$ is ubiquitylated by the KPC (Kip1 ubiquitylation-promoting complex) complex. This E3 complex does not recognize $p27^{KIP}$ as a ubiquitylation substrate unless it is first imported into the nucleus (47).

Phylogenetic distribution and sequence conservation of Ho and yeast *VMA1* inteins coincide with their biological functions and evolutionary history. Ho mediation of mating type switching is a relatively recent innovation of *S. sensu stricto* and close species, most likely occurring 50–70 million years ago (17, 48). Ho proteins are known only in this group and cluster together in phylogenetic analyses (Fig. 6). The closest proteins to Ho are the fungal *VMA1* inteins (49). Besides *S. sensu stricto* these are found in other Saccharomycete yeasts such as *Kluveromyces lactis* (50) and *Candida tropicalis* (51), which split from the *S. sensu stricto* group before the latter acquired the *HO* gene (17, 48). This is further indication regarding the origin of Ho from an intein (15). *VMA1* yeast inteins are also more diverse then Ho proteins (Ref. 48 and Fig. 6) indicating their earlier origin, and probably also reflecting the reduced evolutionary selection they face. Intein genes must efficiently protein-splice to survive (18, 19); their homing capability (mediated by their endonuclease domains) is only necessary for long-term survival and can be inactivated or lost (5, 52–54).

S. castellii includes in addition to its typical *HO* gene a gene coding for a Ho-like protein. This gene has all the Ho protein sequence features: intein protein splicing, LAGLIDADG homing endonuclease, DNA recognition region, and zinc finger domains. It is most similar to the *K. lactis HO* pseudogene (5). Despite its Ho-specific features that include the unique zinc finger domain (whose sequence cannot be used in the phylogenetic analysis with inteins), the *S. castellii* Ho-like protein does not cluster with the typical Ho proteins, nor with the VMA1 inteins (Fig. 6). This protein and the *K. lactis HO*-like pseudogene include sequence regions corresponding to the two Ho NLSs, but lack the basic residues that define these NLSs (not shown). These regions are also not very similar between these two published *HO*-like genes. An *HO*-like gene was recently reported in *K. thermotolerans* and based on this gene and the *K. lactis HO*-like pseudogene an earlier date for appearance of *HO* prior to the branching of *K. lactis* was proposed (5). Further examination of this hypothesis awaits public release of the sequence of the *K. thermotolerans HO*-like gene. Our phylogenetic analysis supports the acquisition of *HO* closer to the appearance of *Z. rouxii* (17, 48). This species branched off before the *Saccharomyces* genome duplication (37) has a typical *HO* gene with both NLS1 and NLS2, and confidently appears as the earliest branch of the known Ho sequences (Fig. 6).

The totally different strategies adopted by Ho and PI-SceI to regulate their activity since diverging from their common ancestor can now be explained at the molecular level. Ho nuclear import is very efficient and involves two NLSs and at least four abundant importins. Both Ho NLSs are conserved in *HO* of all *Saccharomyces* species, but have no apparent parallel in yeast *VMA1* inteins. This suggests that adoption of a new nuclear import strategy occurred very early in the evolution of Ho. The divergence in NLS is supported by the different karyopherins employed by each endonuclease. Whereas PI-SceI nuclear import is mediated by SrpI, Ho is nuclear in *srp1* mutants and needs PseI, Kap123, and Sxm1 for its nuclear import via NLS1, and Kap120 for import via NLS2. The

highly efficient Ho nuclear import is thus a successful strategy for achieving a high rate of mating type switching. Diploidization of yeast cells that have switched mating type enables sporulation in conditions of nutrient deprivation thus increasing fitness of *HO* yeast. *HO* cells that accumulate stable protein within the nucleus suffer from perturbation of the cell cycle (4). We find that the highly efficient nuclear import of Ho has evolved in parallel with equally efficient DDR-mediated Ho nuclear export and ubiquitylation by SCF^{Ufo1} that occurs exclusively in the cytoplasm (3, 4, 6, 7). This promotes degradation of Ho in the proteasome and provides a mechanism for maintaining genome stability. Thus the combination of highly efficient nuclear import together with fortuitous recruitment of functions of the DDR that target Ho to the proteasome for rapid destruction has enabled the establishment of homothallic mating type interconversion.

REFERENCES

1. Herskowitz, I. (1988) *Microbiol. Rev.* **52,** 536–553
2. Cosma, M. P., Tanaka, T., and Nasmyth, K. (1999) *Cell* **97,** 299–311
3. Kaplun, L., Ivantsiv, Y., Kornitzer, D., and Raveh, D. (2000) *Proc. Natl. Acad. Sci. U. S. A.* **97,** 10077–10082
4. Kaplun, L., Ivantsiv, Y., Bakhrat, A., and Raveh, D. (2003) *J. Biol. Chem.* **278,** 48727–48734
5. Fabre, E., Muller, H., Therizols, P., Lafontaine, I., Dujon, B., and Fairhead, C. (2005) *Mol. Biol. Evol.* **22,** 856–873
6. Ivantsiv, Y., Kaplun, L., Tzirkin-Goldin, R., Shabek, N., and Raveh, D. (2006) *Mol. Cell. Biol.* **26,** 1579–1588
7. Kaplun, L., Tzirkin, R., Bakhrat, A., Shabek, N., Ivantsiv, Y., and Raveh, D. (2005) *Mol. Cell. Biol.* **25,** 5355–5362
8. Raveh, D., Hughes, S. H., Shafer, B. K., and Strathern, J. N. (1989) *Mol. Gen. Genet.* **220,** 33–42
9. Jensen, R. E., and Herskowitz, I. (1984) *Cold Spring Harbor Symp. Quant. Biol.* **49,** 97–104
10. Dingwall, C., and Laskey, R. A. (1991) *Trends Biochem. Sci.* **16,** 478–481
11. Gorlich, D., and Kutay, U. (1999) *Annu. Rev. Cell Dev. Biol.* **15,** 607–660
12. Hood, J. K., and Silver, P. A. (1999) *Curr. Opin. Cell Biol.* **11,** 241–247
13. Nash, P., Tang, X., Orlicky, S., Chen, Q., Gertler, F. B., Mendenhall, M. D., Sicheri, F., Pawson, T., and Tyers, M. (2001) *Nature* **414,** 514–521
14. Hirata, R., Ohsumk, Y., Nakano, A., Kawasaki, H., Suzuki, K., and Anraku, Y. (1990) *J. Biol. Chem.* **265,** 6726–6733
15. Pietrokovski, S. (1994) *Protein Sci.* **3,** 2340–2350
16. Bakhrat, A., Jurica, M. S., Stoddard, B. L., and Raveh, D. (2004) *Genetics* **166,** 721–728
17. Butler, G., Kenny, C., Fagan, A., Kurischko, C., Gaillardin, C., and Wolfe, K. H. (2004) *Proc. Natl. Acad. Sci. U. S. A.* **101,** 1632–1637
18. Liu, X. Q. (2000) *Annu. Rev. Genet.* **34,** 61–76
19. Pietrokovski, S. (2001) *Trends Genet* **17,** 465–472
20. Gimble, F. S., and Thorner, J. (1992) *Nature* **357,** 301–306
21. Duan, X., Gimble, F. S., and Quiocho, F. A. (1997) *Cell* **89,** 555–564
22. Russell, D., Jensen, R., Zoller, M., Burke, J., Errede, B., Smith, M., and Herskowitz, I. (1986) *Mol. Cell. Biol.* **6,** 4281–4294
23. Nahon, E., and Raveh, D. (1998) *Nucleic Acids Res.* **26,** 1233–1239
24. Nagai, Y., Nogami, S., Kumagai-Sano, F., and Ohya, Y. (2003) *Mol. Cell. Biol.* **23,** 1726–1736
25. Gimble, F. S. (2000) *FEMS Microbiol. Lett.* **185,** 99–107
26. Uetz, P., Giot, L., Cagney, G., Mansfield, T. A., Judson, R. S., Knight, J. R., Lockshon, D., Narayan, V., Srinivasan, M., Pochart, P., Qureshi-Emili, A., Li, Y., Godwin, B., Conover, D., Kalbfleisch, T., Vijayadamodar, G., Yang, M., Johnston, M., Fields, S., and Rothberg, J. M. (2000) *Nature* **403,** 623–627
27. Longtine, M. S., McKenzie, A., 3rd, Demarini, D. J., Shah, N. G., Wach, A., Brachat, A., Philippsen, P., and Pringle, J. R. (1998) *Yeast* **14,** 953–961
28. Henikoff, S., Henikoff, J. G., Alford, W. J., and Pietrokovski, S. (1995) *Gene* (*Amst.*) **163,** GC17–GC26
29. Morgenstern, B. (1999) *Bioinformatics* **15,** 211–218
30. Felsenstein, J. (1989) *Cladistics* **5,** 164–166
31. Perler, F. B., Olsen, G. J., and Adam, E. (1997) *Nucleic Acids Res.* **25,** 1087–1093

32. Moure, C. M., Gimble, F. S., and Quiocho, F. A. (2002) *Nat. Struct. Biol.* **9,** 764 –770
33. James, P., Halladay, J., and Craig, E. A. (1996) *Genetics* **144,** 1425–1436
34. Leslie, D. M., Zhang, W., Timney, B. L., Chait, B. T., Rout, M. P., Wozniak, R. W., and Aitchison, J. D. (2004) *Mol. Cell. Biol.* **24,** 8487– 8503
35. Leung, S. W., Harreman, M. T., Hodel, M. R., Hodel, A. E., and Corbett, A. H. (2003) *J. Biol. Chem.* **278,** 41947–41953
36. Butler, M. I., and Poulter, R. T. (2005) *Fungal Genet. Biol.* **42,** 452– 463
37. Kurtzman, C. P., and Robnett, C. J. (2003) *FEMS Yeast Res.* **3,** 417– 432
38. Rout, M. P., Blobel, G., and Aitchison, J. D. (1997) *Cell* **89,** 715–725
39. Schlenstedt, G., Smirnova, E., Deane, R., Solsbacher, J., Kutay, U., Gorlich, D., Ponstingl, H., and Bischoff, F. R. (1997) *EMBO J.* **16,** 6237– 6249
40. Sydorskyy, Y., Dilworth, D. J., Yi, E. C., Goodlett, D. R., Wozniak, R. W., and Aitchison, J. D. (2003) *Mol. Cell. Biol.* **23,** 2042–2054
41. Seedorf, M., and Silver, P. A. (1997) *Proc. Natl. Acad. Sci. U. S. A.* **94,** 8590 – 8595
42. Rudra, D., and Warner, J. R. (2004) *Genes Dev.* **18,** 2431–2436
43. Leslie, D. M., Grill, B., Rout, M. P., Wozniak, R. W., and Aitchison, J. D. (2002) *Mol. Cell. Biol.* **22,** 2544 –2555
44. Schaper, S., Franke, J., Meijsing, S. H., and Ehrenhofer-Murray, A. E. (2005) *J. Cell Sci.* **118,** 1473–1484
45. Stage-Zimmermann, T., Schmidt, U., and Silver, P. A. (2000) *Mol. Biol. Cell* **11,** 3777–3789
46. Ghaemmaghami, S., Huh, W. K., Bower, K., Howson, R. W., Belle, A., Dephoure, N., O'Shea, E. K., and Weissman, J. S. (2003) *Nature* **425,** 737–741
47. Kamura, T., Hara, T., Matsumoto, M., Ishida, N., Okumura, F., Hatakeyama, S., Yoshida, M., Nakayama, K., and Nakayama, K. I. (2004) *Nat. Cell. Biol.* **6,** 1229 –1235
48. Koufopanou, V., and Burt, A. (2005) *Mol. Biol. Evol.* **22,** 1535–1538
49. Dalgaard, J. Z., Klar, A. J., Moser, M. J., Holley, W. R., Chatterjee, A., and Mian, I. S. (1997) *Nucleic Acids Res.* **25,** 4626 – 4638
50. Koufopanou, V., Goddard, M. R., and Burt, A. (2002) *Mol. Biol. Evol.* **19,** 239 –246
51. Gu, H. H., Xu, J., Gallagher, M., and Dean, G. E. (1993) *J. Biol. Chem.* **268,** 7372– 7381
52. Telenti, A., Southworth, M., Alcaide, F., Daugelat, S., Jacobs, W. R., Jr., and Perler, F. B. (1997) *J. Bacteriol.* **179,** 6378 – 6382
53. Gimble, F. S. (2001) *Nucleic Acids Res.* **29,** 4215– 4223
54. Posey, K. L., Koufopanou, V., Burt, A., and Gimble, F. S. (2004) *Nucleic Acids Res.* **32,** 3947–3956
55. Hood, J. K., and Silver, P. A. (2000) *Biochim. Biophys. Acta* **1471,** M31–M41
56. Buchnik, R. (2000) *Transport of Ho Endonuclease of Yeast from the Cytoplasm to the Nucleus.* M.Sc. thesis, Ben Gurion University, Beersheba, Israel